Zeros of the 3-state Potts model partition function for the square lattice revisited.

Paul P. Martin*[1] and Siti Fatimah Zakaria†[1,2]

[1]Department of Pure Mathematics, University of Leeds, Leeds, LS2 9JT, United Kingdom
[2]Department of Computational and Theoretical Sciences, International Islamic University Malaysia, 25200 Kuantan, Malaysia

January 23, 2019

Abstract

We compute the exact partition function for the 3-state Potts model on square lattices of several sizes larger than previously accessible. Making comparison with the exactly solved Ising model we show that, for aspects of the analytic structure close to the ferromagnetic transition point, these lattices are large enough to approach the thermodynamic limit. Subject to certain assumptions this allows for computation of estimates for the specific heat critical exponent. We thus obtain an estimate for this exponent. The estimate is consistent with the known result, thus demonstrating the potential use of this method for other models. We also discuss the antiferromagnetic transition.

Keywords: statistical mechanics, Potts model, square lattice, universal critical exponent

This paper is dedicated to the memory of Vladimir. What PM knows of mentoring he learned from Vladimir, his mentor. Hopefully FZ will become another link in the chain.

1 Introduction

We assume familiarity with Potts models on square lattices as toy models exhibiting phase transitions — see for example Wu [28] or [17] (and cf. e.g. Rittenberg [26] and [2–4, 11, 22]). We give formal definitions in § 1.1.

The outline of this paper is as follows. First we compute the exact partition function for the 3-state Potts model on square lattices of several sizes larger than previously accessible. Such a partition function takes the form of a huge polynomial in e^{β}. A good way to present it is to plot the zeros in the complex plane. Then the density of zeros is measured near the transition point. The specific heat critical exponent α is approximated from the zero density function. Many properties of the partition function depend heavily on system size, but this density exponent does not (for sufficiently large size). The 3-state model is not integrable, but by a trustworthy folklore the specific heat exponent is known exactly (see e.g. [3, 29]). Thus this paper obtains an approximation to a number that has been known exactly for many years! So why is it interesting?... It is interesting because the folklore gives very little information about the physics, or about the analytical

*email: p.p.martin@leeds.ac.uk
†email: fatimahsfz@iium.edu.my

'mechanics' of phase transition modelling (cf. for example [7, 8]). The present calculation offers the prospect of an interpolation between the physical approaches such as in [7, 8] and the conformal field theoretic approach [13].

1.1 The Potts model - basic definitions

Fix a spacial dimension d. The Q-state Potts model gives representations of a bulk ferromagnet (depending on the coupling constant) in $\mathbb{R}^d$, in which spins are allowed to be oriented from Q possible spin directions. The physical spins are assumed to sit at a regular collection L of points in some interval of $\mathbb{R}^d$. This *lattice* induces a 'nearest neighbour' graph.

We take $L = \mathbb{Z}^2 \subset \mathbb{R}^2$, or some finite interval thereof; and $Q = 3$. Hence this paper studies the 3-state Potts model on the square lattice. It will be useful to define it slightly more generally.

Definition 1.1. *A graph Λ is a triple $\Lambda = (V, E, f)$ where V, E are sets, and f is a function $f : E \to V \times V$.*

Fix Q a natural number and $\underline{Q} = \{1, 2, ..., Q\}$. Given a set V, a function $\sigma : V \to \underline{Q}$ is called a Q-state Potts spin configuration on V. Let Ω be the set $\hom(V, \underline{Q})$ of all spin configurations.

Definition 1.2. *For given Q the bare Potts Hamiltonian on $\Lambda = (V, E, f)$ is*

$$\mathcal{H} : \hom(V, \underline{Q}) \to \mathbb{Z}$$

given by

$$\mathcal{H}(\sigma) = \sum_{\substack{\langle i,j\rangle = f(e),\\ e \in E}} \delta_{\sigma(i),\sigma(j)}$$

where the Kronecker delta function

$$\delta_{\sigma(i),\sigma(j)} = \begin{cases} 1, & \text{if } \sigma(i) = \sigma(j) \\ 0, & \text{if } \sigma(i) \neq \sigma(j) \end{cases}.$$

Definition 1.3. *For given Q and Λ the Potts partition function is a function of a scalar β defined as*

$$Z(\beta) = \sum_{\sigma \in \hom(V, \underline{Q})} \exp(\beta \mathcal{H}(\sigma)) \tag{1}$$

We may think of $\beta = J/(k_B T)$ in which J is the coupling constant, T is temperature and k_B is Boltzmann's constant. We will not specify physical units, so here only the sign of J is significant.

Let $x = e^{\beta}$. For a given graph Λ, the partition function (1) can be written in polynomial form,

$$Z(\beta) = \sum_{\sigma \in \Omega} x^{\mathcal{H}(\sigma)}. \tag{2}$$

Roughly speaking, the partition function of a single graph is of no use and no interest — unless it is the graph Λ_{lab} corresponding to a laboratory sample of material (but such samples are so big that computing their partition function is impossible). So, what is interesting is properties of the partition function that (a) become stable through a sequence of lattices including Λ_{lab}; (b) correspond to physical observables. There are several subtleties to this statement. For brevity we refer the reader to [17, Ch.11] for these. Here we turn now to our results.

2 Raw results: zeros of partition function

We write $N \times M'$ for the square lattice with periodic boundary condition in the N direction and open boundary condition in the M direction.

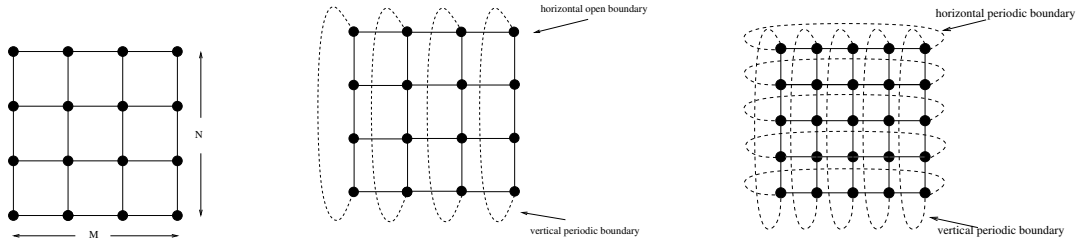

(a) (b) (c)

Figure 1: Square lattices with system size $N \times M$ and different boundary conditions.

Suppose we have 'ferromagnetic' coupling $J > 0$. Then $e^{\beta} \to 1$ as $T \to \infty$. If $T \to 0$ then $e^{\beta} \to \infty$. Thus the $x \in (1, \infty)$ region in this case corresponds to physical states.

On the other hand when $J < 0$ (antiferromagnetic coupling) then $T \to 0$ gives $e^{\beta} \to 0$. Here the $x \in (0, 1)$ region is the physical region.

We compute the partition function by transfer matrix methods; and zeros using a high-precision Newton-Raphson method. In terms of computation it is easier to 'grow' the $N \times M'$ lattice in the M direction than the N direction. Also finite size effects are, in practice, slightly greater with open boundary conditions, where there is a boundary. On the other hand for the analysis we will perform, making the M direction significantly longer than N makes the system into a 'thickened' 1d system rather than 2d (see [17, Ch.11] for details). A practical balance between these considerations is to have M slightly larger than N, and most of our results are for lattices of this type.

The biggest previous result is in [18], with square lattice sizes up to $12 \times 13'$. These were achieved using essentially the same transfer matrix methods as results from almost twenty years earlier (see e.g. [17]), with the increase being due simply to 'Moore's Law'. Since we are interested in sequences of lattices, some of the previous results are reproduced here for comparison. Figure 2 presents the zeros distributions for square lattices with $N = 10, 11, 12$.

Almost another 20 years later, advancement of technology (again simply in the Moore's Law sense) now allows us to extend to bigger lattice sizes. Here new results are shown for $N = 13, 14, 15$. See Figures 3 to 5.

2.1 Preliminary analysis

The circular locus of zeros pinching the ferromagnetic phase transition point is in evidence as before. But two features of the distribution obfusc in earlier results have become manifest.

As we increase the lattice size, the density of zeros close to the physical region increases. The line density near the physical region can now be investigated using the new results. The line density near the phase transition is related to the specific heat universal critical exponent of the phase transition [9, 15, 17]. We will discuss this in more detail in § 3.

Second, while the locus in the antiferromagnetic region remains unclear, we can analyse aspects of the zeros distribution there. If there exist a phase transition, the folklore theory is that it occurs at $x = 0$ [3, 16, 17]. Here, the zeros may form multiple lines, or become dense in some kind of 'cone'-like structure near the real axis.

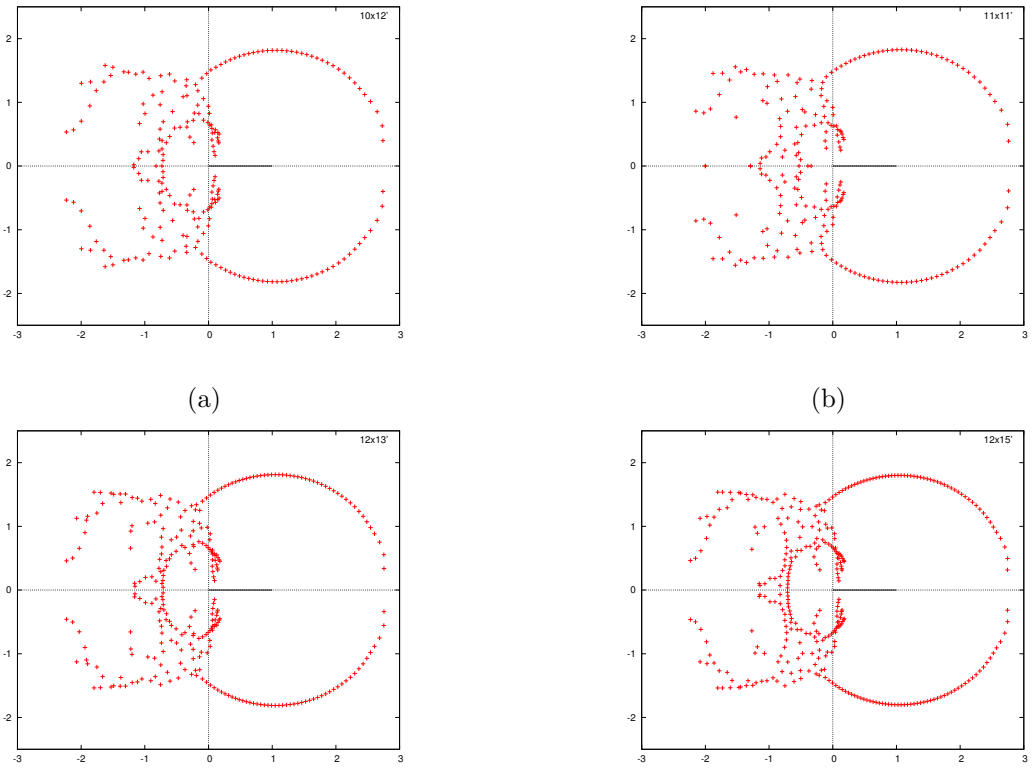

(a) (b)

(c) (d)

Figure 2: Zeros distribution for (a) $10 \times 12'$, (b) $11 \times 11'$, (c) $12 \times 13'$, (d) $12 \times 15'$ square lattices.

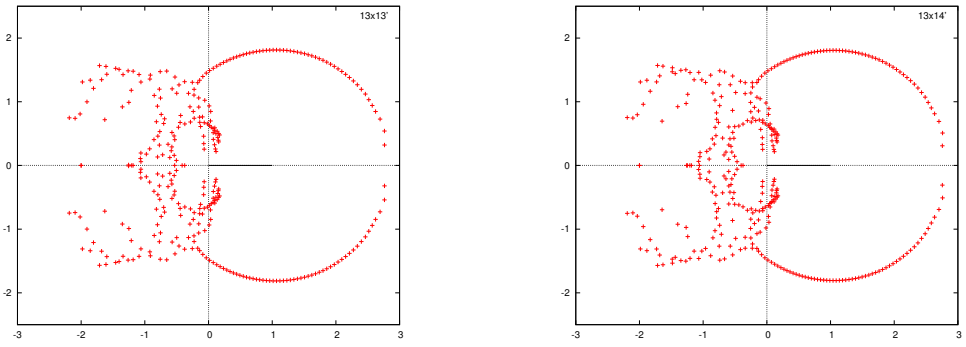

(a) (b)

Figure 3: Zeros distribution for $13 \times 13'$ and $13 \times 14'$ square lattices.

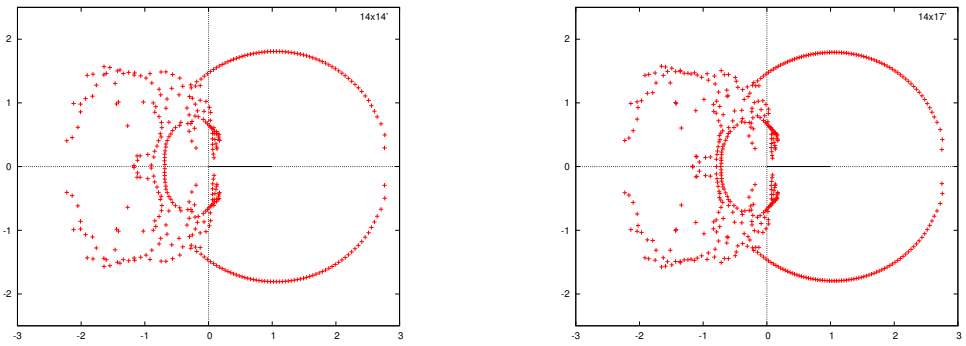

(a) (b)

Figure 4: Zeros distribution for $14 \times 14'$ and $14 \times 17'$ square lattices.

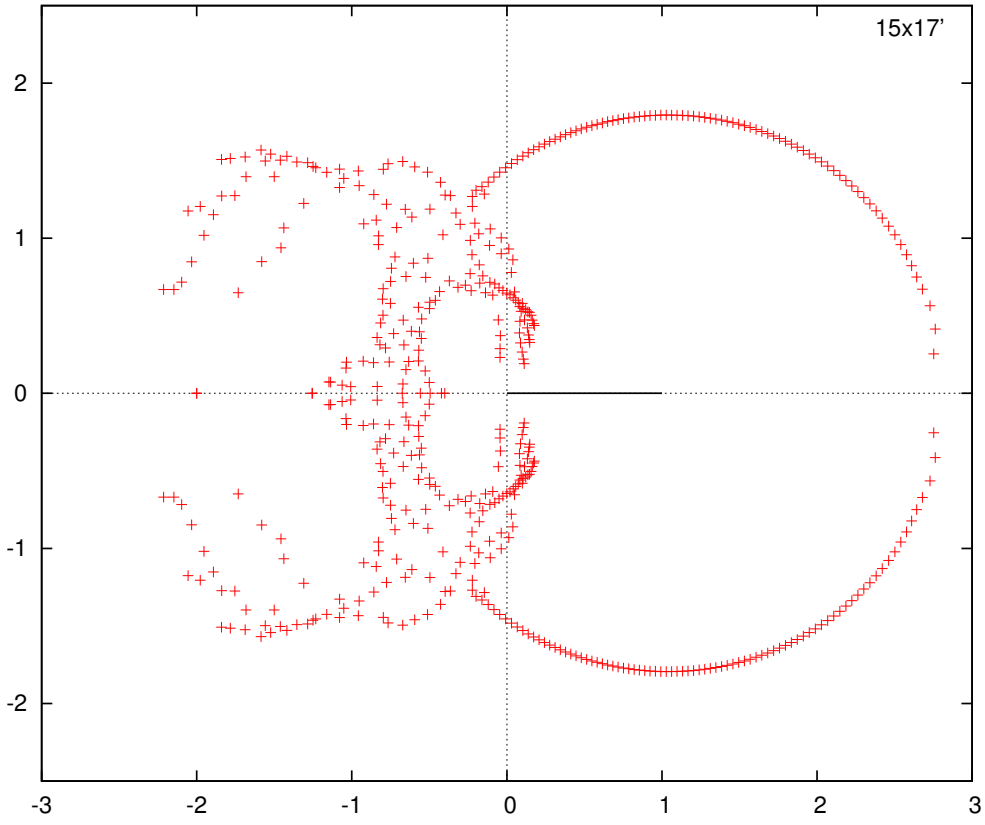

Figure 5: Zeros distribution for $15 \times 17'$ square lattice.

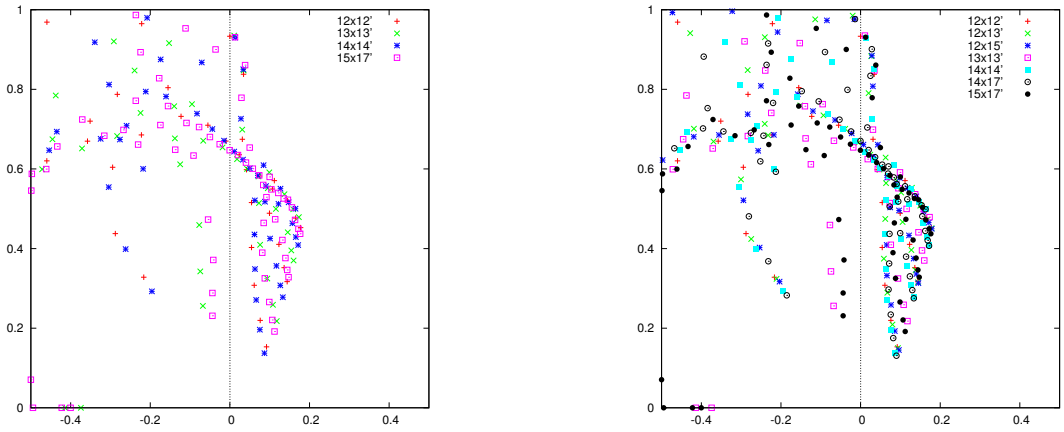

Figure 6: Accumulated zeros distributions close to origin for $N = 12, 13, 14, 15$.

We expect that the closest zeros to the physical axis occur for the largest lattice. Figure 6 shows a subtlety to this. The distribution for different lattice sizes for the (-0.5,0.5)-region is shown in this figure. The closest zeros in this region are given by the square lattice of size $N = 14$, not 15. Comparing the zeros near the real axis for even and odd N suggest that the finite size effect is greater in the antiferromagnetic region than the ferromagnetic region. We shall discuss this in § 5.

2.2 Comparison with Onsager's solution: zero distributions for $Q = 2$

When addressing the question of how to analyse these results, a fresh look at Onsager's exact solution [14, 20] to the square lattice Ising model provides a useful comparison. Onsager's partition function allows us to find the zeros distribution for any square lattice (but in general for boundary conditions different from ours). (It also allows us to take the thermodynamic limit and extract critical exponents directly and exactly — which is the natural and normal approach [1]. But for the (non-integrable) 3-state model this approach is not directly available. Instead here we will look at extracting exponents from 'stable' sequences of finite lattice cases.)

Onsager's partition function is given by [14, 20]

$$Z_{NM} \sim \prod_{k=1}^{N} \prod_{r=1}^{M} \left(\frac{(1+e^{-4\beta})^2}{e^{-2\beta}(1-e^{-4\beta})} - 2(\cos(2\pi k/N) + \cos(2\pi r/M)) \right) . \tag{3}$$

Here $\sim$ means we omit analytically unimportant overall factors, for clarity (cf. e.g. [12, 27]).

For $x = e^{2\beta}$ and $C_{kr} = \cos(2\pi k/N) + \cos(2\pi r/M)$, the vanishing of each factor in (3) becomes:

$$\begin{aligned} \frac{(1+e^{-4\beta})^2}{e^{-2\beta}(1-e^{-4\beta})} - 2(\cos(2\pi k/N) + \cos(2\pi r/M)) &= 0 \\ e^{-8\beta} + 2C_{kr}e^{-6\beta} + 2e^{-4\beta} - 2C_{kr}e^{-2\beta} + 1 &= 0 \\ x^{-4} + 2C_{kr}x^{-3} + 2x^{-2} - 2C_{kr}x^{-1} + 1 &= 0 \\ x^4 - 2C_{kr}x^3 + 2x^2 + 2C_{kr}x + 1 &= 0 . \end{aligned} \tag{4}$$

Note that this factorises as

$$(x^2 + \alpha_+ x - 1)(x^2 + \alpha_- x - 1)$$

where $\alpha_\pm = -C \pm \sqrt{C^2-4}$. The roots of these factors are

$$\frac{-(-C \pm \sqrt{C^2-4}) \hat{\pm} \sqrt{2C(C \mp \sqrt{C^2-4})}}{2} \tag{5}$$

with the hatted $\hat{\pm}$ independent of the others. It follows that the zeros lie on the locus shown in Fig.7(a), and that in the limit they become dense on this locus.

Let us put $M = N$. We are interested in the zeros close to the ferromagnetic transition point, and hence in small values of k, r, for which the quadratic Maclaurin expansion

$$C_{kr} \sim 2 - \epsilon_{kr}$$

where

$$\epsilon_{kr} = \frac{2\pi(k^2+r^2)}{N^2}$$

is good. We have

$$C^2 - 4 = (C+2)(C-2) \sim -4\epsilon_{kr}$$

Substituting in (5) we get

$$\frac{2 \mp 2i\sqrt{\epsilon_{kr}} \hat{\pm} 2\sqrt{2}(1 \mp i\sqrt{\epsilon_{kr}})}{2} \quad \rightsquigarrow \quad (1+\sqrt{2})(1 \mp i\sqrt{\epsilon_{kr}})$$

close to the critical point at $x = 1+\sqrt{2}$. From this we see that the imaginary part is

$$\sim \sqrt{\epsilon_{kr}}$$

while the real part varies much more slowly with k, r. (N.B. This simple analysis was well-known from Onsager's result. But we now use it to test a computation for the exponent which generalises to other models.)

As we will see below, we wish to determine the large-N-asymptotic position dependence of the density of points on the line close to 0 given by the set $\sqrt{\epsilon_{kr}}$ as k, r vary. Note from our analysis that the zeros lie on the loci shown in Fig.7(a) below; and, for sufficiently large lattice, the blow up of the part of the first quadrant very close to the phase transition point is given by Fig.7(b).

Note that this zero distribution is the same up to an overall scale for every sufficiently large lattice. The scale does not affect the exponent (see below), so in this sense this figure gives the thermodynamic limit *even though it is discrete*.

Caveat: Kaufman's boundary conditions are not physical. For physical boundary conditions there cannot be a zero on the positive real axis. However the differences in boundary conditions become irrelevent in the thermodynamic limit, so for us they are simply part of the finite-size effects that we must control in our analysis below.

It might also be interesting to compare with the cubic lattice Ising model. This is not integrable, but see for example [6, 15, 21, 25].

3 Zero density analysis I: theory and benchmarking

In our results above we observe the tendency of the *locus* of zeros to stabilise for larger lattices. This is well-known (if not fully understood). But our progress with computing bigger lattices gives us the opportunity to begin a more sophisticated and useful analysis of the zeros distribution.

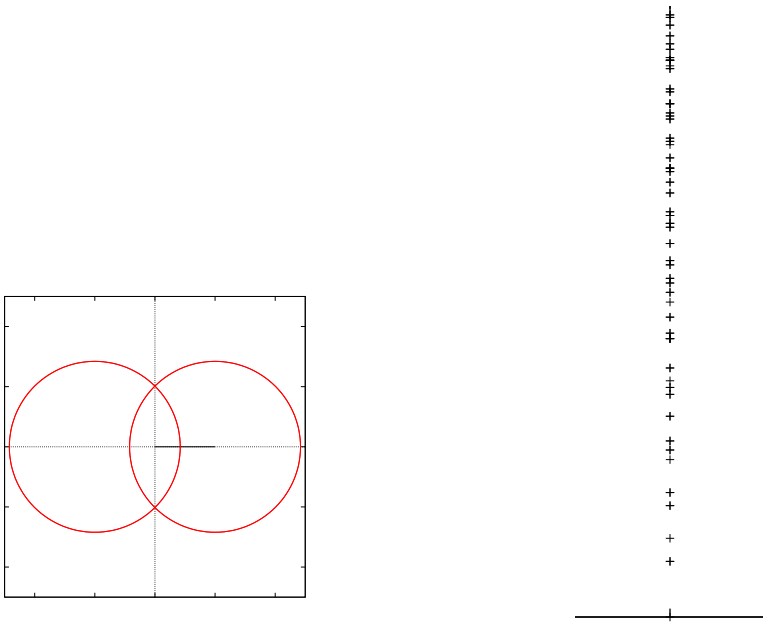

Figure 7: (a) Locus of zeros; (b) zeros close to critical point.

Formally the locus of zeros determines the phase transition points, which could be considered physical. But these are not universal properties, and so are not in practice experimentally quantitatively observable. The most natural observable properties to consider are critical exponents.

The general theory connecting density of zeros to the specific heat critical exponent is given for example in [17, §11.1].

In short, the setup is as follows. [15–17]. Let y denote the distance away from the critical point in the complex plane (note that, for differences, working with x or β is asymptotically the same). Suppose the density of zeros $a(y)$ obeys a power law for small y, that is

$$a(y) \sim |y|^{1-p}. \tag{6}$$

for $0 \leq p < 1$. The specific heat is then given by [17]

$$\frac{dU}{d\beta} \overset{(\beta-\beta_c)\to 0}{\sim} |\beta - \beta_c|^{-p}.$$

This gives the critical exponent $\alpha = p$.

3.1 On zero density in the discrete case

A laboratory sample of a ferromagnet is, of course, not infinite. The physicist's interest in the thermodynamic limit stems from the assumption that laboratory samples are large enough that suitable intensive observables have stopped depending on system size — so that the infinite lattice result is as good as the one we want, the large finite lattice result. So in the present context the question arises: what does the zero density analysis above look like for a finite system that is big enough to be in the limit?

The natural answer is that if we break the complex neighbourhood of the transition point up into several very small finite equal intervals ('bins') and count zeros in the intervals then the

variation as we move away a short distance from the critical point along the line (i.e. in some non-real direction in the complex plane) will discretely reflect the limit dependence. In the *power law* cases of interest this implies that a log-log plot of frequency in a bin against distance from the critical point will (for sufficiently large systems) have a constant gradient; we will get the same gradient for all sufficiently large systems; and the gradient is $m = 1 - \alpha$.

Observe that several conditions must be in place for this to work. In order to have a verifiable constant gradient we need several bins. And to have several bins close to the transition point the bins must be small. But in order for the number of points in a small bin to *not* be small (else we will have discretisation errors) the number of points must be high. So the system must be large. None of these observations gives us quantitative estimates of the size needed. Practical verification must then arise from finding bin sizes that give a constant gradient to high accuracy; and from confirming that this constant is stable with (sufficiently large) system size. (Remark: It seems likely that a system satisfying the former condition will necessarily satisfy the latter. But we will test both.)

Here the data for the log-log graph is obtained as follows. A working assumption is that, sufficiently close to the critical point, the zeros in x lie on a line essentially perpedicular to the real axis. Note from the results above that this is valid in our case (but cf. § 5). In this case the distance y from the critical point can be taken to be given by the imaginary part, and bins constructed accordingly. However for a lattice of finite size there will not be many zeros 'arbitrarily' close to the critical point, in which case the larger scale structure of the locus is relevant to how y is measured. Here the first quadrant in the complex plane is divided into several segments of equal angle from the centre of the circular locus. This is somewhat ad hoc (cf. for example the analysis discussed in [17, §11.1]), but any procedure which constructs essentially similar bins close to β_c is equivalent in the limit. We number the bins $1, 2, ..., b$ from the real axis. The total number of zeros in each bin Δ_i is then counted and plotted against the mid-point value of y in Δ_i, in the log-log plot. We use only the bins closest to the real axis — which we take to be those up to the high point of the circular locus.

Linear regression line fitting is used to fit the log-log plot, and to give a quantitative measure of the quality of linear fit. For various reasons the linear fitting is predicted to work near the transition point (first few bins), and not necessarily further away. But as noted, we do not have a quantitative guide for what 'near' means, so we run the fit until it fails.

3.2 Benchmarking with the Ising model

Here we examine the zeros from Onsager's partition function. For 100×100 square lattice (and others), the log-log plot gives a line distribution as illustrated below. Changing the number of bins (within a range that keeps down discretisation effects) does not greatly affect the log-log graph. The gradient is approximately $m \sim 1$ which gives $\alpha \sim 0$. This observation supports the method, since we know that $\alpha = 0$ for the Ising model (see e.g. [1, 29]).

Fig.9 is the version for a large lattice ($N \geq\sim 1000$) in the asymptotic region using our analysis above. It is interesting to note (for reference below) that the first bin is (very slightly) an outlier, even in the limit.

The very simple but rather beautiful distribution in Fig.7(b) has been discussed many times, in a variety of contexts. See for example [1, 10]. We reiterate that it is of interest to us now for comparison to the $Q = 3$ result. In particular note the irregularity of the pattern on the small scale (which would here defeat a simple analysis of the type proposed in [17, p.294] for example). The $Q = 3$ result, even for much smaller lattices, is much more regular in comparison. The ferromagnetic

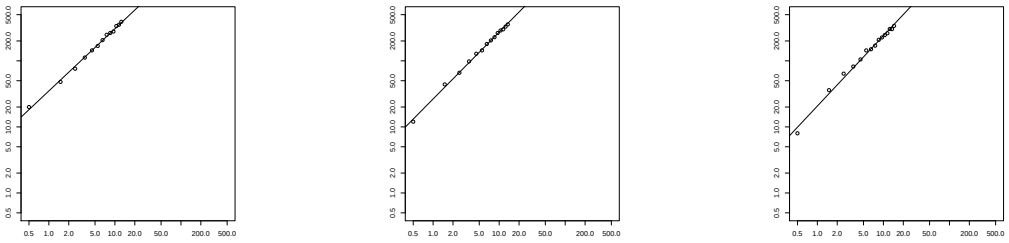

(a) Number of bins, $b = 13$. (b) Number of bins, $b = 14$. (c) Number of bins, $b = 15$.

Figure 8: Lattice size 100×100, $Q = 2$: Bin occupancy and linear regression analysis.

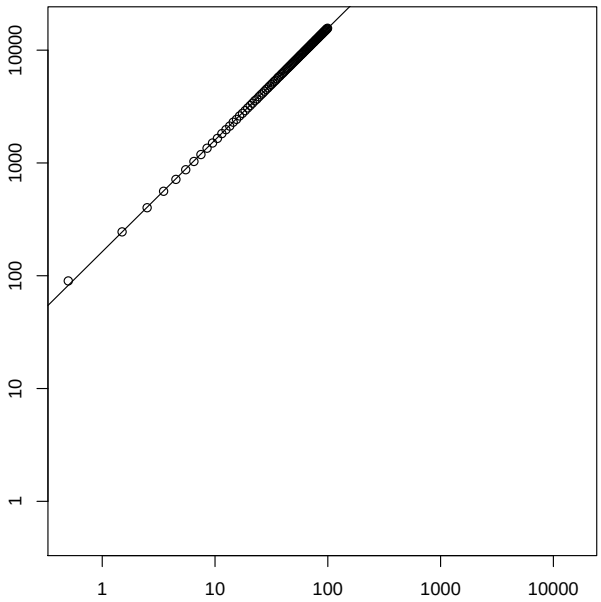

Figure 9: Scaled asymptotic bin occupancy for $Q = 2$, $b = 100$.

loci look superficially similar between $Q = 2$ and 3 because of the large scale geometry, but this shows that they are substantively different. We will develop this point in a separate work.

4 Zero density analysis II: 3-state Potts model

Here we apply the analysis from § 3.1 to the 3-state Potts model zeros distributions. Our first examples use bins radial from the centre of the ferromagnetic circular locus, from the axis to vertical. Firstly for $15 \times 17'$ with number of bins $b = 10, 11, 12$. Note that the first bin can be empty, in which case we omit it — this is ad hoc, but there are plenty of bins:

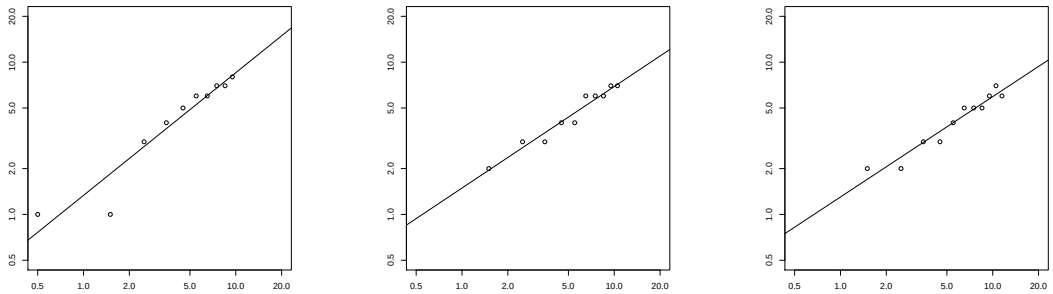

The linear regression fits to these give slope $m = .8, .67, .66$ with standard deviations $.09, .05, .06$ respectively. (Recall that the exact value is $2/3$, giving $\alpha = 1/3$.) Fig.10 gives $N = 14$.

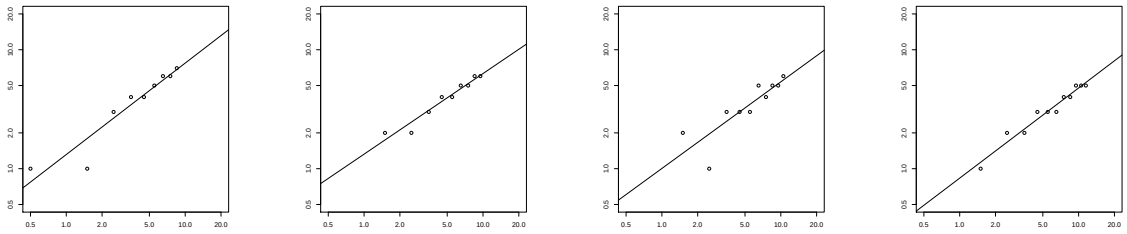

Figure 10: Case $N = 14$, $b = 9 - 12$. Linear fit $m = .77 \pm .1,\ .68 \pm .06,\ .73 \pm .16,\ .76 \pm .05$.

Another way to extract a density from the discrete data, in principle, is to plot the separation of zeros against distance from the critical point. Under suitable circumstances separation is inversely proportional to density. This would not work in the $Q = 2$ case since there is too much fine structure in the distribution. The log-log plot here is in Fig.11. The gradient (with opposite sign due to the inverse) is $.72 \pm .02$. The regression fitted gradient is the same for $N = 15$ and 14, and indeed even the pattern of zeros looks similar, much as happens for the thermodynamic limit Ising model above (although the pattern is intriguingly different between the two models). However the gradient is slightly too high, so there is something very interesting to investigate further here.

To test for finite-lattice sensitivity to the method of division into bins see Figs.12 and 13; and Table 1. These give results using bins radial from the *origin* (b is the number of bins in the positive quadrant, but again we keep only bins meeting the ferromagnetic locus before the high-point of the circle). Several further variants on these plots can be found in [30].

Discussion. We use linear regression to get objective numerical estimates, but even supported by visual checks linear regression on log-log plots is a famously tricky way to extract exponents and

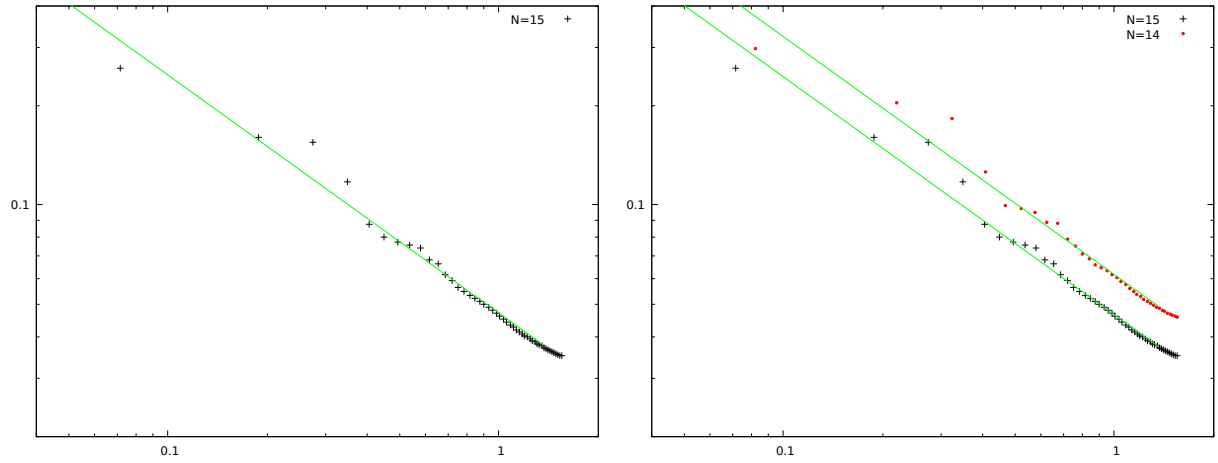

Figure 11: Separation versus locus distance from critical point for $15 \times 17'$ and $14 \times 14'$.

(a) Number of bins, $b = 9$.

(b) Number of bins, $b = 10$.

Figure 12: Lattice size $14 \times 14'$: Linear regression on log-log plots.

(a) Number of bins, $b = 11$.

(b) Number of bins, $b = 12$.

Figure 13: Lattice size $15 \times 17'$: Linear regression on log-log plots.

Table 1: Fitted slope m of log-log plot for $14 \times 14'$ and $15 \times 17'$ square lattices.

Lattice size	$14 \times 14'$			$15 \times 17'$		
Bin, n	Lin. reg.	Std. dev.	Manual	Lin. reg.	Std. dev.	Manual
6	0.5858	0.1611	0.75	0.4933	0.11493	0.6
7	0.7688	0.09357	0.6	0.5344	0.13894	0.8
8	0.69276	0.11134	0.7	0.6109	0.08523	0.7
9	0.67331	0.08984	0.6	0.7027	0.08235	0.6
10	0.74003	0.09145	0.7	0.7116	0.10301	1
11				0.7128	0.04786	0.7
12				0.7047	0.06792	0.7

error bars (there are analogous problems even with experimental data). So there is no claim that the above is a complete engine for computing exponents. Bluntly put, the combined analysis above gives something like $\alpha \sim .3 \pm .1$. But what is interesting is that the numerics are close enough that we can indeed study quantitatively the *way* the analytics manifests the phase transition.

5 On the antiferromagnetic region

For various reasons, such as the complexity of the ground-state, we expect that finite size effects are more severe in the antiferromagnetic region. And in any case it will be evident from the main figures that the locus of zeros is more complex than the ferromagnetic locus. Nonetheless, we can make some interesting observations from our results. The folklore (see e.g. [3]) says that the antiferromagnetic critical point is at temperature $T = 0$. This corresponds to the origin in the complex plane. We now focus briefly on the zero distribution in the neighbourhood of the antiferromagnetic region — the line $(0, 1)$. See Figure 6 for the zeros distribution for the antiferromagnetic neighbourhood, for $N = 12, .., 15$.

In the ferromagnetic region, as the lattice size is increased the closest zeros approach the real axis monotonically. The zeros in the antiferromagnetic region converge to the axis less straightforwardly with system size. However consider the separate even and odd N plots in Figure 14. Each individual sequence in this figure is 'moving closer to' the real axis as the size increases.

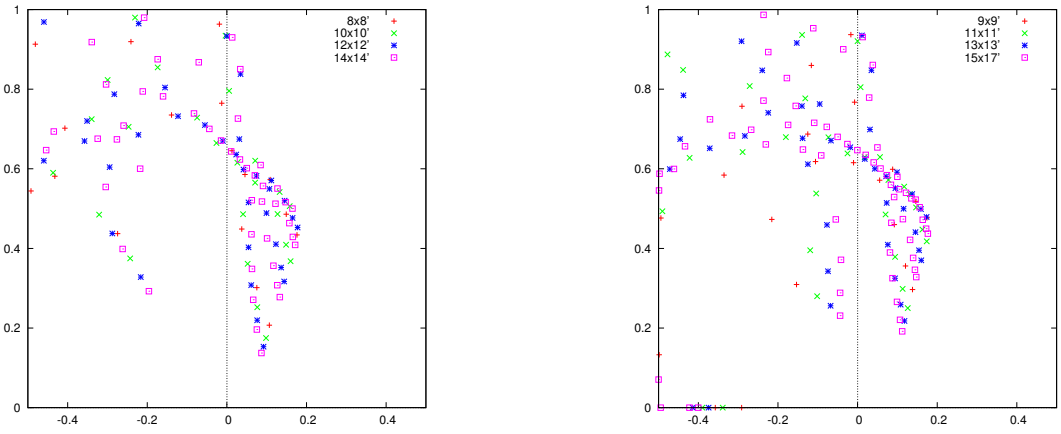

(a) (b)

Figure 14: Antiferromagnetic region for lattice size with a) even N and b) odd N.

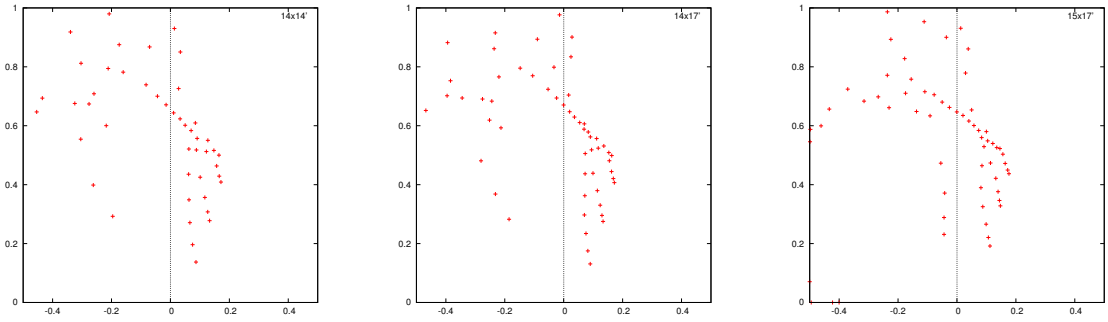

Figure 15: Antiferromagnetic region. Individual cases.

In the Ising model, the antiferromagnetic groundstate is frustrated on small periodic lattices for odd N, and this indeed leads to a parity-dependent size effect. However this kind of alternating groundstate is only one of many for $Q = 3$, and there are other patterns that are frustrated by even N, so it is intriguing that there is a noticable odd/even dependence in our data.

The present data seems unlikely to yield an accurate specific heat exponent. But we can investigate the 'fine structure' in the size dependence.

Observe that in all computed cases there is, for each of the two critical points, a unique complex conjugate pair of zeros closest to it (see e.g. Fig.15). Let the distance from closest zero to critical point be denoted d_f and d_{af} respectively. To separate out the odd/even effect from the size effect, consider the ratio. See Table 2. Note the marked parity dependence. Can we explain this?

Table 2: Closest zeros distance from critical points and their ratio for different N.

N	d_f	d_{af}	$r = d_{af}/d_f$
10	0.436885	0.200684	0.4593520034
11	0.391279	0.280068	0.7157756997
12	0.353739	0.178626	0.5049655254
13	0.322341	0.247607	0.7681523604
14	0.295721	0.162422	0.5492406694
15	0.255333	0.222039	0.8696055739

Write the partition function in the form

$$Z = \sum_{i=0}^{2NM-N} a_i x^i.$$

Thus a_0 is the degeneracy of the antiferromagnetic groundstate. Does this have a significant parity dependence? For a 3-state Potts model on a *one-dimensional* N-site lattice with periodic boundary condition — a ring, the antiferromagnetic ground states are the 'Barlow sequences' (see e.g. [24]), so the degeneracy is given by the Barlow number [23]:

$$b_N = 2^N + 2(-1)^N \text{ for } N > 0. \tag{7}$$

Every ring groundstate induces 2d groundstates in an obvious way (start with the ring as a first layer and add further layers each by applying $+1$ or -1 (mod.3) to the whole ring configuration).

So let us compare the number of antiferromagnetic ground states between the one-dimensional case and the $N \times M'$ lattice case.

We normalise the groundstate multiplicities by expressing them as a fraction of *all* configurations. We make intensive quantities by taking the appropriate root of the ratio. Obviously

$\sqrt[N]{b_N/3^N}$ converges rapidly to 2/3. The odd/even difference is essentially undetectable from about $N = 7$. Table 3 tabulates this with

$$r_M = \sqrt[M]{\frac{a_0}{3^{NM}}} \tag{8}$$

and

$$r_{NM} = \sqrt[N]{r_M}. \tag{9}$$

Table 3: Antiferromagnetic groundstate ratios and roots (here $M = N$ except for $15 \times 17'$).

N	$\sqrt[N]{\frac{b_N}{3^N}}$	a_0	$\frac{a_0}{3^{NM}}$	r_M	r_{NM}
3	0.6057	24	0.00121933	0.1068334089	0.4744994304
4	0.6865	4626	0.000107465	0.1018161711	0.5648773878
5	0.6581	38880	4.59E-008	0.0340674062	0.5087071172
6	0.6700	37284186	2.48E-010	0.0250722546	0.5410020343
7	0.6651	1886476032	7.88E-015	0.0096659433	0.5154395618
8	0.6673	9527634436194	2.77E-018	0.0063885629	0.5317106966
9	0.6663	2825260002442752	6.37E-024	0.0026466285	0.5171690832
10	0.6667	77048019386429374638	1.49E-028	0.0016499225	0.526922027
11	0.6666	132046297983569105731584	2.45E-035	0.000713757	0.5175581207
12	0.6666	196988209730968720770773734 50	3.88E-041	0.0004289582	0.524044193
13	0.6666	193554351965524736352758387687424	4.50E-049	0.0001909958	0.517517353
14	0.6666	159147870862104841838351532192943853490	4.85E-056	0.0001119444	0.5221387133
15	0.6666	29274766481378105714861373681423215500710370344 96	6.32E-074	0.0000494483	0.516349101

Fig.16 shows that the odd/even difference persists for much longer in 2d. This might explain the noted parity difference in the zero distributions, but raises its own questions. Also intriguing is the apparent convergence overall of the 'groundstate density' r_{NM} to a constant around .5. (The final system size is $15 \times 17'$ and hence anomalous in this data set. This is frustrating since its density also looks anomalous. However the calculation takes several months on a supercomputer so it is not a trivial matter to compute $15 \times M'$ for other M.) We will further address these challenges elsewhere.

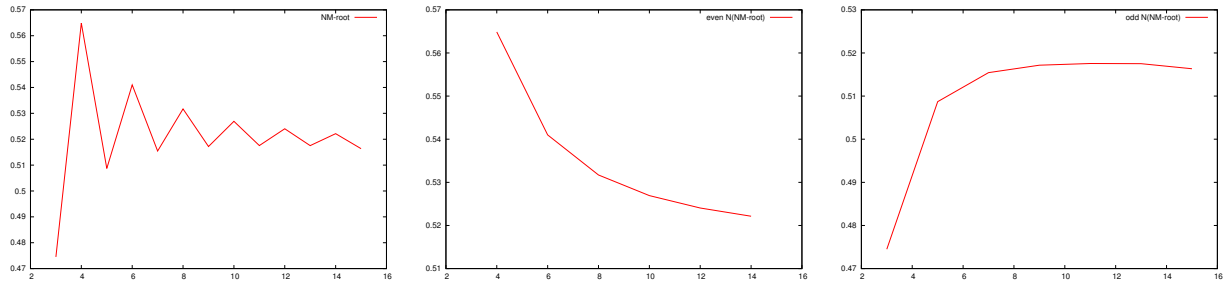

Figure 16: The NM^{th}-roots for (a) all N; (b) even N; (c) odd N.

6 Acknowledgment

The authors thank University of Leeds, PM thanks EPSRC (grant EP/I038683/1), and SFZ thanks International Islamic University Malaysia (RIGS17-051-0626) for partially supporting this manuscript preparation.

References

[1] Abe, R. (1967). Logarithmic singularity of specific heat near the transition point in the Ising model. *Progress of Theoretical Physics*, 37(6):1070–1079.

[2] Baxter, R. J. (1973). Potts model at the critical temperature. *Journal of Physics C: Solid State Physics*, 6(23):L445.

[3] Baxter, R. J. (1982). *Exactly Solved Models in Statistical Mechanics*. Academic Press Limited.

[4] Baxter, R. J. (1995). Solvable model in Statistical Mechanics, from Onsager onward. *Journal of Statistical Physics*, 78(1-2):7–16.

[5] Baxter, R. J. (2011). Onsager and Kaufmans calculation of the spontaneous magnetization of the Ising model. *Journal of Statistical Physics*, 145(3):518–548.

[6] Bhanot, G. and Sastry, S. (1990). Solving the Ising model exactly on a 5x5x4 lattice using the connection machine. *Journal of Statistical Physics*, 60:333–346.

[7] Einhorn, M. B., Savit, R., and Rabinovici, E. (1980). A physical picture for the phase transitions in Z_n symmetric models. *Nuclear Physics B*, 170(1):16 – 31.

[8] Elitzur, S., Pearson, R. B., and Shigemitsu, J. (1979). Phase structure of discrete abelian spin and gauge systems. *Phys. Rev. D*, 19:3698–3714.

[9] Fisher, M. E. (1965). The nature of critical points. In Britten, W. E., editor, *Lectures in Theoretical Physics*, volume 7c, pages 1–159. University of Colorado Press, Boulder.

[10] Flajolet, P. and Vardi, I. (1996). Zeta function expansions of classical constants. `http://algo.inria.fr/flajolet/Publications/landau.ps`.

[11] Hintermann, A., Kunz, H., and Wu, F. Y. (1978). Exact results for the Potts model in two dimensions. *Journal of Statistical Physics*, 19(6):623–632.

[12] Huang, K. (1987). *Statistical Mechanics*. John Wiley & Sons Ltd., second edition.

[13] Huse, D. A. (1984). Exact exponents for infinitely many new multicritical points. *Phys. Rev. B*, 30:3908–3915.

[14] Kaufman, B. (1949). Crystal Statistics. II. Partition function evaluated by spinor analysis. *Phys. Rev.*, 76:1232–1243.

[15] Martin, P. P. (1983). Finite lattice Z(3) models in two and three dimensions. *Nuclear Physics B*, 225(4):497–504.

[16] Martin, P. P. (1985). Potts models and dichromatic polynomials. In Giacomo M. D′Ariano and Mario Rasetti, editors, *Integrable Systems in Statistical Mechanics*, pages 129–142. World Scientific.

[17] Martin, P. P. (1991). *Potts Models and Related Problems in Statistical Mechanics*, volume 5. World Scientific Pub Co Inc.

[18] Martin, P. P. (2000). Zeros of the partition function for the triangular lattice three-state Potts model II. `http://www1.maths.leeds.ac.uk/~ppmartin/ZEROS/pdf/q3tri2x.pdf`.

[19] Martin, P. P. (2007). An introduction to basic statistical mechanics for mathematicians I: Background. `http://www1.maths.leeds.ac.uk/~ppmartin/pdf/SM1-1.pdf`.

[20] Onsager, L. (1944). Crystal Statistics. I. A two-dimensional model with an order-disorder transition. *Phys. Rev.*, 65:117–149.

[21] Pearson, R. B. (1982). Partition function of the Ising model on the periodic 4x4x4 lattice. *Phys. Rev. B*, 26:6285–6290.

[22] Savit, R. (1980). Duality in field theory and statistical systems. *Rev. Mod. Phys.*, 52:453–487.

[23] Sloane, H J A, editor (1964). The on-line encyclopedia of integer sequences. Sequence at. `http://oeis.org/A092297`.

[24] Thompson, R. M. and Downs, R. T. (2001). Systematic generation of all nonequivalent closest-packed stacking sequences of length n using group theory. *Acta Crystallographica*, B57:766–771.

[25] Valani, Y. P. (2011). *On the Partition Function for the Three-dimensional Ising model*. PhD thesis, School of Engineering and Mathematical Sciences, City University, London, United Kingdom.

[26] von Gehlen, G. and Rittenberg, V. (1986). Operator content of the three-state potts quantum chain. *Journal of Physics A: Mathematical and General*, 19(10):L625.

[27] Wannier, G. (1966). *Statistical Physics*. Dover Books on Physics. Dover Publications.

[28] Wu, F. Y. (1982). The Potts model. *Rev. Mod. Phys.*, 54:235–268.

[29] Yeomans, J. M. (1992). *Statistical Mechanics of Phase Transitions*. Oxford University Press.

[30] Zakaria, S. F. (2017). *Analytic Properties of Potts and Ising model Partition Functions and the Relationship between Analytic Properties and Phase Transitions in Equilibrium Statistical Mechanics*. PhD thesis, School of Mathematics, University of Leeds, United Kingdom. http://etheses.whiterose.ac.uk/16323/.